Effects of the human papilloma virus HPV-16 E7 oncoprotein on glycolysis and glutaminolysis: role of pyruvate kinase type M2 and the glycolytic-enzyme complex

Sybille MAZUREK*[1], Werner ZWERSCHKE†‡, Pidder JANSEN-DÜRR†‡ and Erich EIGENBRODT*

*Institute for Biochemistry and Endocrinology, Veterinary Faculty, University of Giessen, Frankfurter Strasse 100, D-35392 Giessen, Germany, †Institute for Biomedical Ageing Research, Austrian Academy of Sciences, Rennweg 10, A-6020 Innsbruck, Austria, and ‡Tiroler Krebsforschungszentrum, Innrain 66, A-6020 Innsbruck, Austria

Proliferating and tumour cells express the glycolytic isoenzyme, pyruvate kinase type M2 (M2-PK), which occurs in a highly active tetrameric form and in a dimeric form with low affinity for phosphoenolpyruvate. The switch between the two forms regulates glycolytic phosphometabolite pools and the interaction between glycolysis and glutaminolysis. In the present study, we show the effects of oncoprotein E7 of the human papilloma virus (HPV)-16 (E7)-transformation on two NIH 3T3 cell strains with different metabolic characteristics. E7-transformation of the high glycolytic NIH 3T3 cell strain led to a shift of M2-PK to the dimeric form and, in consequence, to a decrease in the cellular pyruvate kinase mass-action ratio, the glycolytic flux rate and the (ATP + GTP)/(UTP + CTP) ratio, as well as to an increase in fructose 1,6-bisphosphate (FBP) levels, glutamine consumption and cell proliferation. The low glycolytic NIH 3T3 cell strain is characterized by high pyruvate and glutamine consumption rates and by an intrinsically large amount of the dimeric form of M2-PK, which is correlated with high FBP levels, a low (ATP + GTP)/(CTP + UTP) ratio and a high proliferation rate. E7-transformation of this cell strain led to an alteration in the glycolytic-enzyme complex that correlates with an increase in pyruvate and glutamine consumption and a slight increase in the flow of glucose to lactate. The association of phosphoglyceromutase within the glycolytic-enzyme complex led to an increase of glucose and serine consumption and a disruption of the linkage between glucose consumption and glutaminolysis. In both NIH 3T3 cell lines, transformation increased glutaminolysis and the positive correlation between alanine and lactate production.

Key words: metabolome, nucleotide diphosphate kinase, nucleotides, phosphoglyceromutase, phosphometabolites.

INTRODUCTION

In comparison with most normal proliferating cells, tumour cells have to meet certain metabolic requirements. In particular, they must be capable of sustained cell proliferation under unfavourable conditions, such as a poor supply of oxygen and glucose, as is the case in solid tumours [1–3]. For these requirements, tumour cells are able to regenerate energy either by glycolysis under hypoxic conditions or by glutaminolysis in the presence of oxygen [1–3]. To co-ordinate the different metabolic pathways with oxygen and glucose supply, proliferating cells express a particular isoenzyme of pyruvate kinase (EC 2.7.1.40), called pyruvate kinase type M2 (M2-PK). M2-PK occurs in a tetrameric form with a high affinity for its substrate phosphoenolpyruvate (PEP), and a dimeric form with a low PEP affinity [4,5]. The glycolytic phosphometabolite, fructose 1,6-bisphosphate (FBP), induces the reassociation of the dimeric to the tetrameric form. Serine, which is synthesized from 3-phosphoglycerate and glutamate, activates M2-PK, whereas several other amino acids, such as alanine and proline, which are directly linked to the glutaminolytic pathway, inhibit M2-PK [5]. The interaction between glucose and glutamine metabolism is further modulated by the means by which hydrogen, produced in the glycolytic glyceraldehyde-3-phosphate dehydrogenase (GAPDH) reaction, is transported into the mitochondria [6–8]. The two possibilities for hydrogen transport are the malate–aspartate shuttle and the glycerol 3-phosphate shuttle [4]. In addition, the first evidence shows that the association of phosphoglyceromutase (PGM) type B (EC 5.4.2.1) within the glycolytic-enzyme complex can alter the interaction between glutaminolysis and glycolysis [9]. The glycolytic-enzyme complex is a labile structure formed from a variety of glycolytic enzymes and other constituents [6,8]. The current available data suggest a regulatory function for this complex [9,10–15]. The tetrameric form of M2-PK and the glycerate 2,3-bisphosphate-independent PGM are associated within the glycolytic-enzyme complex, whereas the dimeric form of M2-PK and the glycerate 2,3-bisphosphate-dependent PGM are not [4,6–9]. For PGM, it was shown that transformation of rat oval cells induces the release of PGM out of the glycolytic-enzyme complex [9].

During tumour formation, the tissue-specific isoenzymes of pyruvate kinase, such as L-pyruvate kinase in liver and M1-type pyruvate kinase in muscle and brain, are lost and M2-PK is expressed [4,5]. All tumour cells so far analysed express a high amount of the dimeric form of M2-PK with low-affinity for PEP [4,5,7,16,17]. M2-PK was shown to be directly targetted by certain oncoproteins, such as $pp60^{v-src}$ kinase [18,19] and the E7 oncoprotein of the human papilloma virus (HPV) type 16

Abbreviations used: BCS, bovine-calf serum; DMEM, Dulbecco's modified Eagle's medium; HPV, human papilloma virus; E7, E7 oncoprotein of the HPV-16; FBP, fructose 1,6-bisphosphate; GAPDH, glyceraldehyde-3-phosphate dehydrogenase; hg-NIH, high glycolytic NIH 3T3 cells; lg-NIH, low glycolytic-NIH cells; LDH, lactate dehydrogenase; M2-PK, pyruvate kinase type M2; NDPK, nucleotide diphosphate kinase; PGM, phosphoglyceromutase; PEP, phosphoenolpyruvate.

[1] To whom correspondence should be addressed (e-mail Sybille.Mazurek@vetmed.uni-giessen.de).

(E7) [16]. Both oncoproteins lead to a promotion of the dimeric form of M2-PK in cells with high glycolytic flux rates. The expression of E7 in *ras*-expressing rat kidney cells leads to an induction of cell proliferation, a promotion of the dimeric form of M2-PK, a decrease in the ATP/ADP ratio and an upregulation of FBP levels [16].

The inhibition of the lower part of the glycolytic pathway leads to an increase in the glycolytic phosphometabolites, e.g. FBP, and to an increased channelling of the glucose carbon atoms to nucleic acid synthesis [4,5,16]. This metabolic feature can induce severe energy imbalance, because the flow of glucose to FBP consumes ATP before ATP is regained by the flow of FBP to pyruvate [5,20–24]. Therefore in proliferating, and especially in tumour cells, the flow of glucose to FBP and from FBP to pyruvate must be balanced with energy production from glutaminolysis in an exact manner [2,4].

In addition, cell proliferation is an energy consuming process. To prevent cell death from nutrient limitation, several metabolites, such as AMP, FBP and 5-phosphoribosyl-α-pyrophosphate, directly interfere with the protein kinase cascade regulating cell proliferation [4,7].

During the establishment of immortal cell populations from primary mouse fibroblasts by a 3T3 protocol, different cell strains can be derived which differ markedly in their metabolic characteristics [25]. In particular, such experiments yield cell strains with intrinsically differing glycolytic rates, varying between low and high [25]. Although these alterations most likely originate from differences in stochastic events during spontaneous immortalization, no data are available concerning the genetic and/or biochemical changes that are involved. In the present study, we analysed the ability of E7 to transform high glycolytic NIH 3T3 (hg-NIH) cells as opposed to low glycolytic NIH 3T3 (lg-NIH) cells. Both cell strains are efficiently transformed by E7. Although E7 expression allows growth of both cell types in soft agar, the proliferation rate of hg-NIH cells in monolayer culture is considerably enhanced, whereas that of lg-NIH cells is not altered by E7. Furthermore, E7 expression has quite distinct effects on metabolic parameters in both cell types. We found that in lg-NIH cells, in contrast to hg-NIH cells, the dimeric form of M2-PK was dominant, and that in hg-NIH cells expression of the E7 protein led to a shift of the tetrameric form of M2-PK to the dimeric form, but in lg-NIH cells E7 expression did not induce a further increase in the content of the dimeric form of M2-PK. In both hg-NIH and lg-NIH cells, expression of E7 triggered a considerable increase in the flux from glutamine to lactate, whereas it affected the glycolytic flux rates differently.

MATERIALS AND METHODS

Cell lines

hg-NIH cells (early-passage NIH 3T3 cells, which have a high aerobic glycolytic rate) were used after stable transfection with the pMo expression vector (1/M cells) [26] or with expression vectors encoding wild-type HPV-16 E7 (E7/2 cells) [26,27]. lg-NIH cells (low glycolytic, wild-type NIH 3T3 cell line) were obtained from A.T.C.C. (Rockville, MD, USA). Early passage cells with a low glycolytic rate, were co-transfected with expression vectors for pJ4Ω16E7WT or with empty vector [28], and a hygromycin resistance gene. E7-expressing stable transfectants were derived by selection in hygromycin-containing medium.

Cell culture

Cell lines were cultivated in Dulbecco's modified Eagle's medium (DMEM) (Sigma, Deisenhofen, Germany), supplemented with 2 mM glutamine, 100 units penicillin/ml, 100 μg streptomycin/ml and bovine-calf serum (BCS) [10,29]. For flux measurements, the cells were arrested in DMEM containing 0.5 % (v/v) BCS for 48 h, washed twice in DMEM and then released into DMEM medium containing 0.5 % (v/v) BCS. The supernatants were analysed 4 h after release. For all other experiments DMEM containing 10 % (v/v) BCS was used. Since enzyme activities and metabolite concentrations are dependent on cell density, for all gel-permeation and isoelectric-focusing experiments, and for metabolite and nucleotide determinations, only preparations with the same mean cell density were used. In the case of the flux measurements, cell density was taken into account in the statistical analysis [7,30].

Transformation experiments

Cells were grown in DMEM supplemented with 10 % fetal-calf serum, 2 mM L-glutamine and 100 μg streptomycin/ml, and transfected, as described previously [27,28], with 10 μg of each plasmid and 1 μg of an expression vector for the hygromycin gene by calcium phosphate co-precipitation [29]. The cells were then placed under hygromycin selection (200 μg/ml) for 2 weeks. Hygromycin-resistant colonies were harvested and analysed for E7 expression by Western blotting. E7-expressing cell lines were seeded into 0.3 % (w/v) low-melting agarose (SeaPlaque Agarose; Biozyme, Hessisch Oldendorf, Germany), and colonies were counted 3 weeks later.

Determination of generation time

Cells were counted at different time points (t_1, t_0) using a Neubauer Chamber. The logarithm of the cell number (N) was plotted against the time (t), and the generation time (g) was calculated as follows:

ν (growth rate) $= \lg N_1 - \lg N_0 / 0.43429 \times (t_1 - t_0)$

Hence, $g = 1/\nu$.

Western-blot analysis

Immunoblots were performed as described in [7,16]. The monoclonal anti-E7 antibody (clone ED17) was obtained from Santa Cruz Biotechnology and the monoclonal anti-M2-PK antibody (clone DF4) from ScheBo·Biotech AG (Giessen, Germany).

Gel permeation

Cells were extracted in a lysis buffer [100 mM Na_2HPO_4/NaH_2PO_4 (pH 7.4), 1 mM dithiothreitol, 1 mM NaF, 1 mM 2-mercaptoethanol, 1 mM ϵ-aminocaproic acid, 0.2 mM PMSF and 10 % (v/v) glycerol]. The extracts were passed over a gel-permeation column (Sephadex G-200; Pharmacia, Freiburg, Germany), and the activities of M2-PK and, as molecular-mass markers, GAPDH, PGM and enolase, were determined in the fractions as described previously [30,31].

Isoelectric focusing

Cells were extracted with a homogenization buffer containing 10 mM Tris/HCl (pH 7.4), 1 mM NaF and 1 mM 2-mercaptoethanol. Isoelectric focusing was carried out with a linear gradient of glycerol [50–0 % (v/v)] and ampholines (pI 3.5–10.5) as described previously [8].

Flux measurements

Cell culture supernatants were collected at different cell densities and immediately frozen in liquid nitrogen. Glucose, pyruvate,

lactate, glutamine, glutamate, serine and alanine were measured in the supernatants of the cells as described previously [7,30,31].

Nucleotide and metabolite measurements

The cells were extracted with 0.6 M $HClO_4$, the extracts were centrifuged at 40000 ***g*** for 20 min at 4 °C, and the supernatants were collected and neutralized with ice-cold KOH. The supernatants were centrifuged again, divided into four aliquots and freeze-dried. Fructose 1,6-bisphosphate, phosphoenolpyruvate and pyruvate levels were determined enzymically, as described previously [7,31]. Nucleotides were measured by reverse-phase ion-pair liquid chromatography on a Hypersil ODS (5 μm) column (CS-Chromatography Service GmbH, Langerwehe, Germany), as described previously [20].

Statistical analysis

For the glycolytic and glutaminolytic flux measurements, statistical analyses were performed using the statistical program package BMDP [32]. For comparison of the different cell groups, one-way analysis of covariance, with cell density as the covariable, was performed. For those variables dependent on cell density, an adjustment to the mean common cell density was performed and flux rates were described as adjusted means. If the distribution of the measured variables was normal, the arithmetic mean ($\bar{x}$) $\pm$ S.E.M. were used in data. For distributions skewed to the right, a logarithmic transformation of the data was performed and the results are presented as geometric mean and dispersion factor ($\bar{x}_g \cdot$D.F.$^{\pm 1}$). This is the de-logarithmic form of the arithmetic mean ($\pm$S.D.) of the previously logarithmically transformed data. In all other cases, the Student's *t* test was employed.

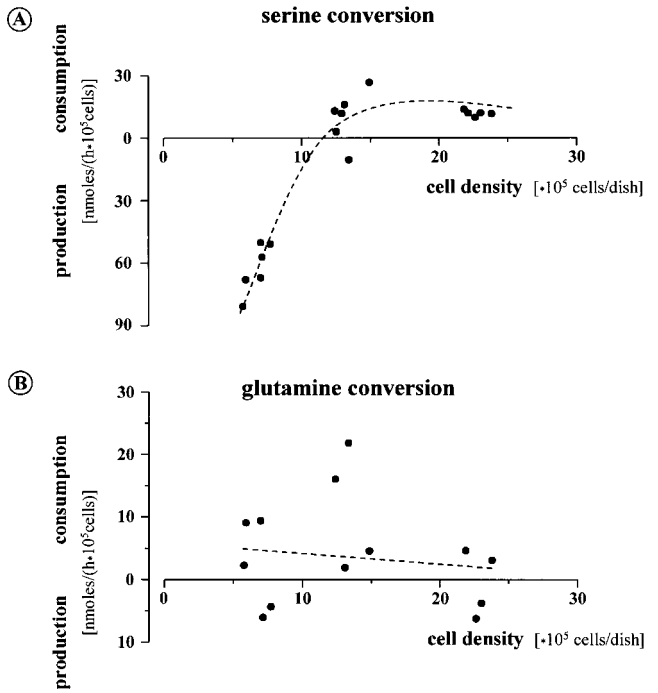

Figure 1 Relationship between serine conversion and cell density (A) and glutamine conversion and cell density (B) in non-transformed hg-NIH cells

Values shown are 10^5 cell density/dish and the production/consumption of serine or glutamine is expressed as nmol/h per 10^5 cells.

RESULTS

Metabolic characterization of hg-NIH and lg-NIH cells

In both NIH 3T3 cell strains, the fluxes of nutrients through the glycolytic and glutaminolytic pathways were reconstructed from measurements of rates of consumption and synthesis for selected key compounds. It is well established that both pathways are the main sources for energy, pyruvate and lactate in cultured cells [1,7–9,30]. For flux measurements, two forms of calculations were chosen. The first calculation was nmoles/h per 10^5 cells, and describes the consumption or production of a certain metabolite by each cell (Figure 1 and Table 1). The second calculation was nmoles/h per dish, and allows detection of possible correlations between the conversion rates of the different metabolites (see Figure 5 and Tables 2a and 2b) [7–9,30]. The combination of these calculations provides an individual metabolic characterization of each cell strain, and is outlined below.

In the hg-NIH cells, the glycolytic flux measurements revealed high rates of glucose consumption and lactate production (Table 1). In lg-NIH cells, the amount of glucose consumed was only 25 % of that consumed in hg-NIH cells. Lactate production of lg-NIH cells was 30 % of that produced in hg-NIH cells (Table 1).

We also addressed the functional linkage between glucose consumption and lactate production. In glycolysis, one mol of glucose is converted into two mol of lactate; therefore, the molar ratio between lactate production and glucose consumption indicates the amount of glucose that is converted to lactate. When glucose consumption was plotted against lactate production in hg-NIH cells, a close linkage between these parameters could be shown (Table 2a). The slope of the regression line was 1.78, with a correlation coefficient (*r*) of 0.892. This value approaches the maximum value of 2 for the ratio of lactate production/glucose consumption, indicating that most of the glucose consumed (89 %) is converted to lactate. In the lg-NIH cell strain, the ratio between lactate production and glucose consumption was decreased to 1.12 with a correlation coefficient of 0.850 (Table 2b). Therefore, in lg-NIH cells, only 56 % of the glucose consumed was converted to lactate. The remaining 44 % must have been used for synthetic processes, such as DNA synthesis.

An inhibition of the pyruvate kinase reaction reduces the availability of glycolytic pyruvate and increases the flow of the glucose carbons to synthetic processes above pyruvate kinase (Scheme 1) [4,5]. The lack of glycolytic pyruvate can be compensated for by the consumption of pyruvate from the medium or by pyruvate produced from glutamine or glutamate degradation. Pyruvate is required for the glutaminolytic production of lactate and, under optimal conditions, one mol of pyruvate is converted into one mol of lactate. In both cell strains, we found a strong correlation between pyruvate consumption and lactate production (hg-NIH cells, $r = 0.860$; lg-NIH cells, $r = 0.962$) (Tables 2a and 2b). When one mol of pyruvate is converted into one mol of lactate, the slope of the regression line is 1.0 when pyruvate consumption (abscissa) is plotted against lactate production (ordinate). A slope value greater than 1.0 indicates that less pyruvate is converted to lactate and that more lactate is derived from sources other than pyruvate.

The consumption of glutamine, which is another source of pyruvate production, was also analysed. We found that glutamine consumption was higher in lg-NIH cells than in hg-NIH cells (Table 1). The correlation coefficients for the ratio between lactate production and glutamine consumption indicated that in

Table 1 Nutrient fluxes in hg-NIH and lg-NIH cells

Results are given as $\bar{x}_g \cdot DF^{\pm 1}$ or $\bar{x} \pm$ S.E.M. (see Statistical analysis in the Material and methods section). *, $P < 0.05$; **, $P < 0.01$; ***, $P < 0.001$; $n = 15$. Results of the statistical comparison of non-transformed hg-NIH cells with non-transformed lg-NIH cells: glucose consumption, $P < 0.001$; lactate production, $P < 0.001$; pyruvate consumption, $P < 0.001$; glutamine consumption, not significant; glutamate production, not significant.

	hg-NIH		lg-NIH	
Metabolites	Non-transformed	E7-transformed	Non-transformed	E7-transformed
Glucose consumption	45.7 · 1.1	28.8 · 1.1*	11.5 · 1.1	7.1 · 1.1**
Lactate production	83.2 · 1.1	53.7 · 1.1**	26.9 · 1.1	17.7 · 1.1**
Pyruvate consumption	10.8 · 1.0	8.6 · 1.0***	7.8 · 1.0	15.7 · 1.0***
Glutamine consumption	0.4 ± 3.1	5.5 ± 3.2	5.2 ± 3.0	17.1 ± 3.3**
Glutamate production	0.5 · 1.2	0.6 · 1.2	0.5 · 1.2	0.1 · 1.2***

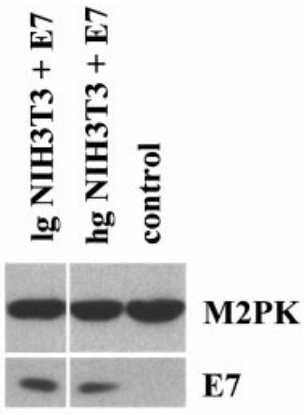

Figure 2 Expression of E7 in lg-NIH and hg-NIH cell lines

Expression of the transfected E7 proteins (lg NIH3T3 + E7 and hg NIH3T3 + E7; bottom panels) was determined by immunoblotting. Expression of M2-PK, which is not influenced by E7 [16], was used to test for equal loading (top panels).

lg-NIH cells ($r = 0.722$) more glutamine was converted to lactate than in the hg-NIH cells ($r = 0.132$) (Tables 2a and 2b).

Interestingly, lg-NIH cells have a shorter generation time than hg-NIH cells, indicating that, in this system, a low rate of glycolysis was associated with enhanced cell proliferation (Table 3). This is probably due to an increase in the degradation of glutamine to lactate, the alternative way of energy production in tissue culture cells (Tables 1 and 2b).

Transformation of NIH 3T3 cells by E7

It has been shown in many previous studies that E7 can transform rodent fibroblasts [16,26,33–35]; however, the metabolic status of the recipient cells was not determined in these studies. Whereas hg-NIH cells can be readily transformed by E7 (Table 3) [27], it is unclear, so far, if lg-NIH cells can also be transformed by E7. To address these questions, E7 was expressed in lg-NIH cells by transfection with an E7-expression vector in combination with a hygromycin-resistance gene. Stable clones were derived and tested for E7 expression (Figure 2 and Table 3); subsequently, cells were cultured in soft agar and the number of colonies were determined. As was shown previously [27], expression of E7 in hg-NIH cells (subclone 1/M) gave rise to a substantial number of colonies, which were not observed in control experiments using either an empty expression vector or vectors expressing transformation-deficient E7 mutants (Table 3) [27]. When lg-NIH cells were transfected with the E7-expression vector, again a substantial number of colonies grew in soft agar, indicating that E7 also transforms lg-NIH cells (Table 3). In this system, expression of E7 led to an induction of cell proliferation in hg-NIH cells but did not detectably alter the proliferation rate of lg-NIH cells (Table 3).

Effect of E7 expression on M2-PK structure and activity

As described previously, in hg-NIH cells expression of the E7 protein led to a shift of the tetrameric form of M2-PK to the dimeric form [16]. To investigate the effect of E7 expression on M2-PK in lg-NIH cells, we first of all compared M2-PK activities in the non-transformed NIH 3T3 cell strains. When the V_{max} of M2-PK was compared in the two strains, no differences were found between lg-NIH and hg-NIH cells (results not shown). In the hg-NIH cells, the tetrameric form of M2-PK was predominant, whereas the lg-NIH cells contained more dimeric M2-PK (Figure 3A). In lg-NIH cells, which are characterized by a high amount of the dimeric form of M2-PK, E7 expression did not induce a further increase in the content of the dimeric form of M2-PK (percentage of the dimeric form in non-transformed lg-NIH cells, 62 ± 4.0; in E7-transformed lg-NIH cells, 62 ± 2.0; $\bar{x} \pm$ S.E.M., $n = 4$).

Effect of E7 expression on the glycolytic-enzyme complex

The activity of several enzymes in the glycolytic pathway is co-ordinately regulated through their physical association in a complex, referred to as the 'glycolytic-enzyme complex' [6–15]. To determine differences in the glycolytic-enzyme complex between hg-NIH and lg-NIH cells, isoelectric focusing was used to analyse the association of these enzymes. Proteins associated within the glycolytic-enzyme complex focus at a common isoelectric point that is different from the isoelectric point of the purified individual proteins. Migrations of proteins inside or outside the glycolytic-enzyme complex are reflected by shifts in their isoelectric points [6,8,9].

In hg-NIH cells, a glycolytic-enzyme complex with the tetrameric form of M2-PK, glycerate 2,3-bisphosphate-dependent PGM type B, enolase (EC 4.2.1.11), GAPDH (EC 1.2.1.12), lactate dehydrogenase (LDH) (EC 1.1.1.27) as well as nucleotide diphosphate kinase (NDPK) type A (EC 2.7.4.6) and adenylate

Table 2 Correlations between the conversion rates of different metabolites

Correlations between different metabolite conversions in non-transformed and E7-transformed hg-NIH and lg-NIH cells. For these calculations, the first metabolite (abscissa) (nmoles/h per dish) was plotted against the second metabolite (ordinate) (nmoles/h per dish) (see Figure 5). Intercept, nmoles/h per dish; $n = 15$. For hg-NIH cells, PK mass-action ratio = 102 PGM (inside the complex); PK mass-action ratio = 66 PGM (outside the complex). For lg-NIH cells, PK mass-action ratio = 55 PGM (outside the complex); PK mass-action ratio = 117 PGM (inside the complex).

(a) hg-NIH cells

		Non-transformed			E7-transformed		
Abscissa	Ordinate	Slope	Intercept	r	Slope	Intercept	r
Glucose	Lactate	1.78	67	0.892	1.68	206	0.916
Pyruvate	Lactate	8.23	−478	0.860	9.90	−558	0.966
Glutamine	Lactate	0.63	1035	0.132	3.11	1352	0.699
Glucose	Glutamine	0.12	64	0.277	0.33	−120	0.739
Serine	Glucose	0.78	638	0.841	2.55	1911	0.833
Serine	Lactate	1.69	1215	0.915	1.22	1035	0.735
Pyruvate	Alanine	0.11	33	0.369	0.66	−25	0.910
Alanine	Lactate	15.49	304	0.454	13.21	80	0.936

(b) lg-NIH cells

		Non-transformed			E7-transformed		
Abscissa	Ordinate	Slope	Intercept	r	Slope	Intercept	r
Glucose	Lactate	1.12	226	0.850	1.75	55	0.710
Pyruvate	Lactate	2.72	100	0.962	2.25	−263	0.890
Glutamine	Lactate	0.42	483	0.722	0.48	241	0.593
Glucose	Glutamine	1.54	−363	0.707	0.80	−29	0.260
Serine	Glucose	0.15	242	0.260	0.50	528	0.725
Serine	Lactate	0.22	493	0.281	1.14	1156	0.664
Pyruvate	Alanine	0.27	71	0.436	0.13	−50	0.798
Alanine	Lactate	1.97	289	0.433	13.41	84	0.872

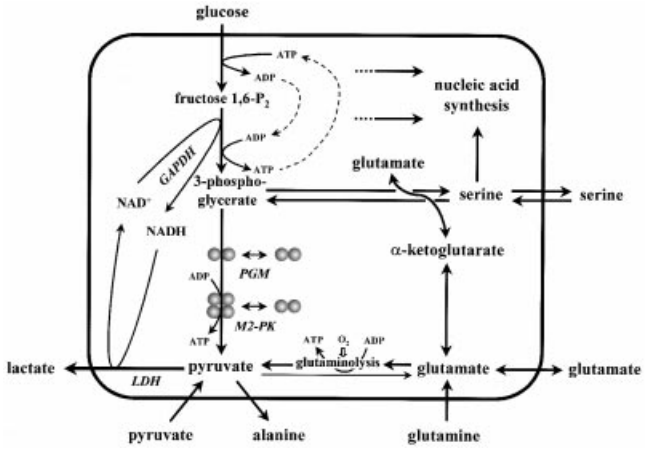

Scheme 1 Overall view of the metabolic interactions

When PGM and M2-PK are associated within the glycolytic-enzyme complex, glucose is mainly converted to lactate and serine consumption increases with increasing glucose consumption. When PGM and M2-PK are not associated within the glycolytic-enzyme complex, all phosphometabolites above M2-PK accumulate and are then available for synthetic processes, such as nucleic acid synthesis. In this case, 3-phosphoglycerate is converted to serine, and glutaminolysis increases with increasing glucose consumption.

kinase (EC 2.7.4.3) was found (Figure 4A) [6]. The dimeric form of M2-PK focused outside the complex [6]. In contrast to the non-transformed hg-NIH cells, in non-transformed lg-NIH cells PGM was not part of the glycolytic-enzyme complex (Figures 4A and 4C). In hg-NIH cells, the expression of the E7 protein

Table 3 Transformation of NIH 3T3 cell types by E7

The different NIH 3T3 cell lines were assayed for colony formation in soft agar, and three independent clones were analysed in each case. Colony formation efficiency for the hg-NIH 3T3 cell line (previously referred to as E7/2 [32]) was set to 100% (++++).

Cell line	Colony formation (%)	Generation time (h)
hg-NIH	–	30.0
hg-NIH + E7	++++	22.9
lg-NIH	–	22.8
lg-NIH + E7	+++	23.8

induced the release of PGM from the complex, whereas PGM migrated into the complex upon expression of E7 in lg-NIH cells (Figures 4B and 4D).

Furthermore, lg-NIH cells were characterized by higher GAPDH and lower NDPK type A activities compared with hg-NIH cells (results not shown). The coupling of M2-PK and adenylate kinase within the glycolytic-enzyme complex regulates AMP levels [4,7,36]. NDPK couples the ATP/ADP ratio with other nucleotide triphosphates [4]. To elucidate the metabolic consequences of these enzymic alterations, we have further investigated the main nutrient parameters.

Effects of E7 on glycolytic and glutaminolytic flux rates

In hg-NIH cells, glycolytic and glutaminolytic flux measurements revealed that the E7-induced promotion of the dimeric form of

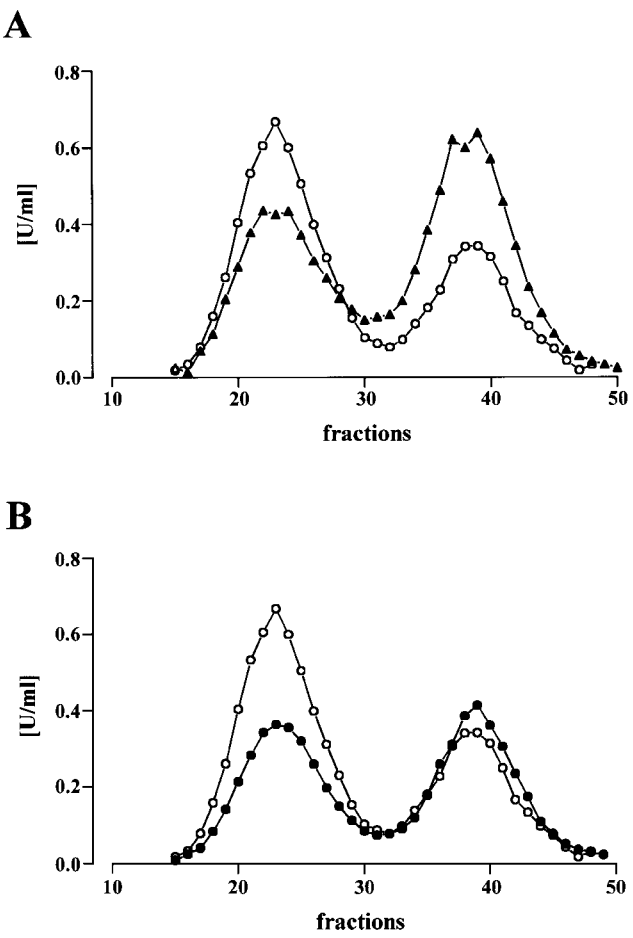

Figure 3 Fractionation by gel permeation of M2-PK in non-transformed hg-NIH and lg-NIH cells (A) and in E7-transformed hg-NIH cells (B), indicating the quaternary structure

The results are of gel permeations of the cytosolic cell extracts. As internal molecular-mass markers, the activities of GAPDH (160 kDa), enolase (100 kDa), and PGM (60 kDa) were measured in each gel-permeation experiment. Percentage of the dimeric form ($\pm$S.E.M., $n = 4$): non-transformed hg-NIH (**A**, **B**, ○), 37 ± 0.6; E7-transformed hg-NIH (**B**, ●), 53 ± 0.8; non-transformed lg-NIH (**A**, ▲), 62 ± 4.0; E7-transformed hg-NIH 62 ± 2.0 (not shown on Figure, but given for comparison).

M2-PK was correlated with a decrease in the glycolytic flux rate, as well as an increase of the flow of glutamine to lactate (glutaminolysis) and pyruvate to lactate (Figure 3B; Tables 1 and 2a). In addition, the expression of E7 led to a release of PGM from the glycolytic-enzyme complex (Figure 4B), with distinct consequences on serine and glutamine metabolism. In non-transformed hg-NIH cells with PGM inside the glycolytic-enzyme complex, serine conversion was strongly influenced by cell density, whereas glutamine conversion was only weakly influenced by cell density (Figures 1A and 1B). The correlation of these parameters indicates that, in non-transformed hg-NIH cells, the association of PGM within the glycolytic-enzyme complex led to a strong linkage between glucose consumption and serine conversion ($r = 0.841$) as well as between serine conversion and lactate production ($r = 0.915$), which indicates a conversion of serine to lactate (Table 2a). The positive correlation between glucose and serine consumption means that serine consumption increased with increasing glucose consumption. When no glucose was consumed, or at very low rates of glucose consumption, serine was produced. On the other hand, the linkage between glucose consumption and glutamine consumption was weak in non-transformed hg-NIH cells (Table 2a). In E7-transformed hg-NIH cells with PGM outside the glycolytic-enzyme complex, the correlation between lactate production and serine conversion was reduced from 1.69 ($r = 0.915$) to 1.22 ($r = 0.735$), whereas the interaction between glucose and glutamine consumption increased from 0.12 ($r = 0.277$) to 0.33 ($r = 0.739$) (Table 2a).

In lg-NIH cells, E7 expression led to a further inhibition of M2-PK, as indicated by the increase of pyruvate and glutamine consumption (Table 1 and Table 2b). However, a further promotion of the dimeric form of M2-PK could not be detected by gel-permeation (see legend to Figure 3). The flow of glucose to lactate slightly increased from 56% to 88% after E7-transformation (calculated from Table 2b). This compensation of the E7-induced inhibition of M2-PK is presumably caused by the reassociation of PGM within the glycolytic-enzyme complex, which increases the flow of 3-phosphoglycerate to phosphoenolpyruvate (Figure 4D). Indeed the mass-action ratio of M2-PK increased in E7-transformed lg-NIH cells (Table 4).

In accordance with non-transformed hg-NIH cells, in E7-transformed lg-NIH cells the re-integration of PGM led to profound alterations in the interaction between glucose, glutamine and serine conversion (Table 2b).

In E7-transformed lg-NIH cells, the correlation between glucose consumption and serine conversion increased from $r = 0.260$ in non-transformed lg-NIH cells to $r = 0.725$ in E7-transformed cells (Table 2b), which indicates that serine consumption increased with increasing glucose consumption. The correlation between lactate production and serine conversion increased from $r = 0.281$ in non-transformed cells to $r = 0.664$ in E7-transformed lg-NIH cells (Table 2b), which indicates a conversion of serine to lactate. Similarly to non-transformed hg-NIH cells, where PGM was also part of the glycolytic-enzyme complex, in E7-transformed lg-NIH cells, the strong linkage between glucose and glutamine consumption was reduced from $r = 0.707$ in non-transformed cells to $r = 0.260$ in E7-transformed cells (Table 2b). The release of alanine was not influenced by the alterations in PGM and the glycolytic-enzyme complex in either cell strain (Figure 5 and Tables 2a and 2b).

Whereas glycolysis produces lactate, in glutaminolysis both lactate and alanine are produced (Scheme 1) [1,2,4,5]. In both NIH 3T3 cell lines, transformation by E7 strongly increased the correlation between alanine and lactate production (Figure 5 and Tables 2a and 2b). Furthermore, the reduction in the intercept of the regression line indicated that alanine was already being produced when lactate production was very low (Figure 5 and Tables 2a and 2b).

Effect of E7 expression on metabolite and nucleotide levels

In hg-NIH cells, the PK mass-action ratio, calculated as [pyruvate]·[ATP]/[PEP]·[ADP], decreased after E7-transformation, reflecting the promotion of the dimeric form of M2-PK after E7-transformation in this cell line (Figure 3B and Table 4). Because of the inactivation of M2-PK, FBP levels increased in E7-transformed hg-NIH cells (Table 4). The (ATP + GTP)/(UTP + CTP) ratio decreased after E7-transformation, and was correlated with an increase in the proliferation rate (Tables 3 and 4). In the non-transformed lg-NIH cells, the very low value of the PK mass-action ratio reflected the high amount of the dimeric form of M2-PK that was already present in this cell line in the absence of E7 (Table 4). Due to the high amount of the dimeric

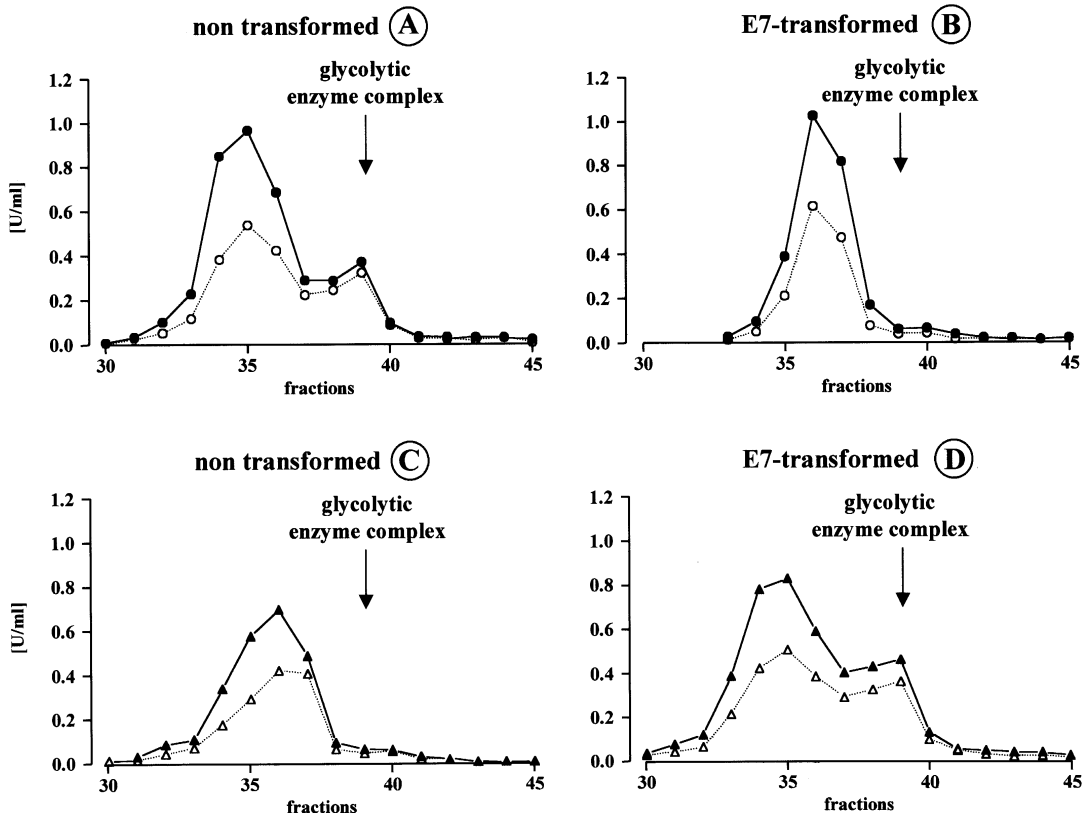

Figure 4 Migration of PGM inside and outside the glycolytic-enzyme complex in non-transformed and E7-transformed hg-NIH and lg-NIH cell strains

Results of isoelectric focusing experiments with cytosolic cell extracts. (**A**) Non-transformed hg-NIH cells, (**B**) E7-transformed hg-NIH cells, (**C**) non-transformed lg-NIH cells, (**D**) E7-transformed lg-NIH cells. The glycolytic-enzyme complex is marked by arrows and consisted of the tetrameric form of M2-PK, the glycerate 2,3-bisphosphate-independent PGM type B, enolase, LDH, GAPDH, adenylate kinase and NDPK type A [6]. ● and ▲, PGM type B measured in the presence of glycerate 2,3-bisphosphate; ○ and △, PGM type B measured in the absence of glycerate 2,3-bisphosphate.

Table 4 Intracellular nucleotide and metabolite levels in hg-NIH and lg-NIH cells

The values shown are nmol/h per 10^5 cells (means ± S.D.; $n = 5$). PK mass-action ratio = [pyruvate]·[ATP]/[PEP]·[ADP]. ***, $P < 0.001$; **, $P < 0.01$; *, $P < 0.05$.

	hg-NIH		lg-NIH	
Metabolites	Non-transformed	E7-transformed	Non-transformed	E7-transformed
FBP	0.22 ± 0.04	0.40 ± 0.04*	0.5 ± 0.2	0.5 ± 0.2
PEP	0.3 ± 0.2	0.4 ± 0.2	1.2 ± 0.2	0.4 ± 0.1***
Pyruvate	2.1 ± 0.2	2.8 ± 0.8	7.1 ± 1.4	6.0 ± 1.6
ATP/ADP	11.1 ± 2.4	9.7 ± 2.4	10.3 ± 5.2	8.1 ± 3.3
AMP	0.5 ± 0.4	0.3 ± 0.3	1.7 ± 1.5	0.05 ± 0.09
GTP/GDP	8.1 ± 3.3	9.8 ± 5.4	7.7 ± 1.9	17.4 ± 11.9
(ATP + GTP)/(UTP + CTP)	4.9 ± 2.6	3.2 ± 0.6	3.7 ± 2.1	2.3 ± 1.1
PK mass-action ratio	102	66	55	117

form of M2-PK, these cells also contained higher FBP levels than the non-transformed hg-NIH cells (Table 4).

Although gel permeation revealed no effect of E7-expression in lg-NIH cells, we noticed a substantial increase in the PK mass-action ratio in E7-transformed lg-NIH cells (Table 4). This may reflect an activation of the pyruvate kinase reaction by increased substrate availability by the re-integration of PGM into the glycolytic complex or by changes in other parameters that remain to be determined. Accordingly, PEP levels decreased in E7-transformed lg-NIH cells, but FBP levels did not increase (Table 4). The (ATP + GTP)/(UTP + CTP) ratio was lower in lg-NIH cells than in hg-NIH cells, which were also characterized by a higher proliferation rate than the hg-NIH cells (Table 3). In lg-NIH cells, E7 expression led to a decrease in the (ATP + GTP)/(UTP + CTP) ratio but had no further effect on the cell proliferation rate (Table 3).

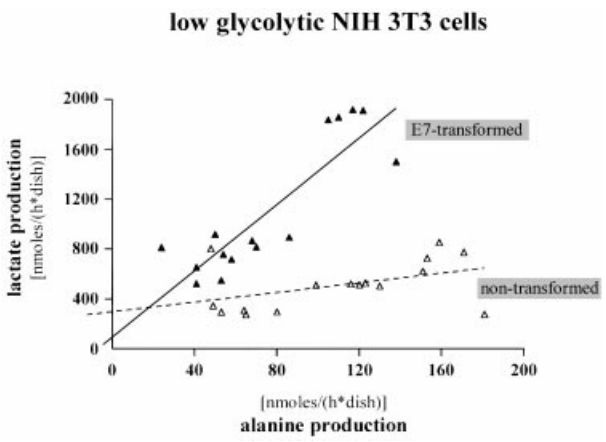

Figure 5 Relationship between alanine and lactate production in non-transformed (△) and E7-transformed (▲) lg-NIH cells

See Table 2(b). Lactate or alanine production is shown as nmol/h per dish.

DISCUSSION

Interaction between glycolysis and glutaminolysis

In accordance with studies in cell culture and solid tumours, M2-PK is the main regulator of the interaction between glycolysis and glutaminolysis [1,2,4–9]. In lg-NIH cells, which were also characterized by a high glutaminolytic flux rate, the dimeric form of M2-PK was predominant, whereas in the hg-NIH cells with a low glutaminolytic flux rate, a high amount of the tetrameric form was found (see Figure 3A and Table 1). E7-transformation of the hg-NIH cells led to a promotion of the dimeric form of M2-PK, a reduction in the glycolytic flux rate and an increase in glutaminolysis (Figure 3B and Tables 1 and 2a).

Co-ordinating glycolysis and glutaminolysis: a role for the glycolytic-enzyme complex

In the present study, we showed, for the first time, that besides the tetramer/dimer ratio of M2-PK and the hydrogen shuttles, the organization of the glycolytic-enzyme complex also plays an important role in the co-ordination of glycolysis, serine metabolism and glutaminolysis [7–9].

The interaction between glycolysis, serine metabolism and glutaminolysis takes place at the level of pyruvate and 3-phosphoglycerate. 3-Phosphoglycerate is reduced to 3-hydroxypyruvate and is transaminated, with glutamate as NH_2 donor, to serine (Scheme 1) [37]. Pyruvate is transaminated with glutamate to alanine [1,4]. Glutamate is the central intermediate of glutaminolysis [2,5]. The end product of glycolysis is lactate, whereas, in glutaminolysis, lactate, serine and alanine are produced (Scheme 1).

Both serine synthesis from glucose and serine degradation to lactate are directly linked to 3-phosphoglycerate, the substrate of PGM [4,37–39]. In solid tumours, degradation of the amino acid glutamine to lactate (glutaminolysis) and the degradation of the amino acid serine to lactate (serinolysis) are found (Scheme 1) [1]. The regulation of these pathways by nutrient supply in solid tumours is different. Glutaminolysis is primarily regulated by the oxygen supply, and serinolysis by glucose supply. Serine production and its release from cells has the function of an energy buffer when the flow of glucose to 3-phosphoglycerate exceeds the flow from 3-phosphoglycerate to pyruvate by pyruvate kinase for the following reasons. In glycolysis, at first ATP is consumed for the synthesis of FBP before energy is regained by the flow of FBP to pyruvate. Net ATP synthesis occurs only with the flow of 3-phosphoglycerate to pyruvate by the pyruvate kinase reaction (Scheme 1) [21–23]. Besides mitochondrial glutaminolysis, the pyruvate kinase reaction is the only means by which proliferating cells can regenerate ATP [1,2,4]. The association of PGM within the glycolytic-enzyme complex allows flexible regulation of the interaction of serinolysis and glutaminolysis with glycolysis [4,9].

Flexible modulation of glycolysis and glutaminolysis by E7

Besides the remarkable differences in the metabolic responses to E7 transformation in both NIH 3T3 cell strains, there were also some interesting similarities which contribute to the transformation potential of the E7 protein in both cell lines [40,41]. These common effects were directly linked to the inhibition of M2-PK by E7. In both NIH 3T3 cell lines, E7-induced inhibition of M2-PK led to an increased flow from glutamine to pyruvate and lactate followed by a strong linkage between pyruvate consumption and alanine production (Tables 2a and 2b). In both NIH 3T3 cells lines, transformation by E7 strongly increased the correlation between alanine and lactate production (Figure 5 and Tables 2a and 2b).

An increased rate of alanine production is correlated with the metastasizing potential of tumour cells [1,42]. Furthermore, in solid tumours, alanine is released and a high correlation between alanine and lactate production is found [1]. An increase in the glutaminolytic flux rate is consistently observed during tumour formation, which is independent of the molecular mechanism by which tumour formation is induced [4,9].

Role of metabolic changes for cell proliferation and transformation

A high concentration of the dimeric form of M2-PK, induced by E7 expression in hg-NIH cells or by an unknown mechanism in lg-NIH cells, was correlated with a high rate of cell proliferation (Figure 3 and Table 3). On the metabolite level, a high concentration of the dimeric form of M2-PK was correlated with high levels of glycolytic phosphometabolites, such as FBP, and an increased channelling of phosphometabolites to nucleic acid and NAD(P)(H) synthesis as well as a high NAD(P)(H)/NAD(P) ratio (Figure 3 and Table 4) [4,7,43–45]. FBP is a potent activator of protein biosynthesis [46]. AMP lowers the NAD(P) levels and the NADH/NAD ratio [4,7]. It has been suggested that the intracellular ratio of NAD(P)H/NAD(P) regulates tyrosine phosphorylation and influences diverse cellular pathways, such as the functions of telomerase and p53 [4,7,43,45]. In lg-NIH cells, E7 transformation led to no further promotion of the dimeric form of M2-PK, and to no further increase in FBP levels and synthetic processes. It seems that in non-transformed lg-NIH cells the synthetic capacity has reached its upper limit, which might explain why, in lg-NIH cells, as opposed to hg-NIH cells, no further enhancement of the cell-proliferation rate was found after E7 transformation.

In accordance with these metabolic relationships, in yeast cells, overexpression of pyruvate kinase leads to a total inhibition of cell proliferation, which can be reactivated by a simultaneous overexpression of protein kinase MCK, which phosphorylates and inactivates pyruvate kinase [47]. The increase in glycolytic phosphometabolite pools by promotion of the dimeric form of M2-PK must be exactly balanced by the flow of glucose to FBP and serine and glutamine metabolism. To ensure this co-

ordination, the tetramer/dimer ratio of M2-PK is allosterically regulated by glycolytic phosphometabolites, such as FBP, or amino acids that link glutaminolysis with glycolysis, such as serine and alanine [1–5]. Another mechanism is the flexible association of PGM within the glycolytic-enzyme complex [9]. Because of the close linkage between glucose and glutamine consumption in non-transformed lg-NIH cells, energy production should be totally disturbed when PGM is not associated within the glycolytic-enzyme complex and when, additionally, M2-PK is shifted to the dimeric form after E7 expression (Table 2b). It is reasonable that only those E7-transformed cell clones of lg-NIH cells can survive when PGM is within the glycolytic-enzyme complex, which leads to an increased flow from 3-phosphoglycerate to PEP and to an increased PK mass-action ratio (Figure 4D) [48]. By the reassociation of PGM with the glycolytic-enzyme complex in E7-transformed lg-NIH cells an increase in AMP levels and an imbalance in the (ATP+GTP)/(UTP+CTP) ratio is prevented (Figure 4D) [4,16,49]. Studies with different cell lines revealed a correlation between the (ATP+GTP)/(UTP+CTP) ratio and cell proliferation [49]. There are indications that PGM associated within the glycolytic-enzyme complex is phosphorylated on histidine and is independent of glycerate 2,3-bisphosphate [6]. Within the glycolytic-enzyme complex, PGM is activated by NDPK type A, presumably by direct phosphate transfer [6]. Therefore the primary inhibition of M2-PK by E7 may lead to alterations in the (ATP+GTP)/(CTP+UTP) ratio, and may lead to a reassociation of PGM within the glycolytic-enzyme complex by the NDPK reaction.

This work was supported by the Land Hessen (Hessisches Ministerium für Wissenschaft und Kunst, HSP III and the Deutsche Forschungsgemeinschaft) to S.M., and by the Austrian Science Funds (FWF), the European Union (Biomed 2) and the Austrian Ministry of Science and Traffic to P.J.-D. We thank Bianca Kulik for excellent technical assistance. This work is dedicated to Erika Dietz who died of cancer in December 1999.

REFERENCES

1 Eigenbrodt, E., Kallinowski, F., Ott, M., Mazurek, S. and Vaupel, P. (1998) Pyruvate kinase and the interaction of amino acid and carbohydrate metabolism in solid tumors. Anticancer Res. **18**, 3267–3274
2 McKeehan, W. L. (1982) Glycolysis, glutaminolysis and cell proliferation. Cell Biol. Int. Rep. **6**, 635–650
3 Freitas, I., Baronzio, G. F., Bono, B., Griffini, P., Bertone, V., Sonzini, N., Magrassi, G. R., Bonandrini, L. and Gerzeli, G. (1997) Tumor interstitial fluid: Misconsidered component of the internal milieu of a solid tumor. Anticancer Res. **17**, 165–172
4 Mazurek, S., Boschek, C. B. and Eigenbrodt, E. (1997) The role of phosphometabolites in cell proliferation, energy metabolism, and tumor therapy. J. Bioenerg. Biomembr. **29**, 315–330
5 Eigenbrodt, E., Gerbracht, U., Mazurek, S., Presek, P. and Friis, R. (1994) Carbohydrate metabolism and neoplasia: New perspectives for diagnosis and therapy. In Biochemical and Molecular Aspects of Selected Cancers, 2, (Pretlow, T. G. and Pretlow, T. P., eds.), pp. 311–385, Academic Press, New York
6 Mazurek, S., Grimm, H., Wilker, S., Leib, S. and Eigenbrodt, E. (1998) Metabolic characteristics of different malignant cancer cell lines. Anticancer Res. **18**, 3275–3282
7 Mazurek, S., Michel, A. and Eigenbrodt, E. (1997) Effect of extracellular AMP on cell proliferation and metabolism of breast cancer cell lines with high and low glycolytic rates. J. Biol. Chem. **272**, 4941–4952
8 Mazurek, S., Hugo, F., Failing, K. and Eigenbrodt, E. (1996) Studies on associations of glycolytic and glutaminolytic enzymes in MCF-7 cells: Role of p36. J. Cell. Physiol. **167**, 238–250
9 Mazurek, S., Eigenbrodt, E., Failing, K. and Steinberg, P. (1999) Alterations in the glycolytic and glutaminolytic pathways after malignant transformation of rat liver oval cells. J. Cell. Physiol. **181**, 136–146
10 Srere, P. A. and Knull, H. R. (1998) Location – location – location. Trends Biochem. Sci. **23**, 319–320
11 Low, P. S., Rathinavelu, P. and Harrison, M. L. (1993) Regulation of glycolysis via reversible enzyme binding to the membrane protein, band 3. J. Biol. Chem. **268**, 14627–14631
12 Clegg, J. S. and Jackson, S. A. (1990) Glucose metabolism and the channeling of glycolytic intermediates in permeabilized L-929 cells. Arch. Biochem. Biophys. **278**, 452–460
13 Engel, M., Seifert, M., Theisinger, B., Seyfert, U. and Welter, C. (1998) Glyceraldehyde 3-phosphate dehydrogenase and Nm23-H1/Nucleoside diphosphate kinase A. J. Biol. Chem. **273**, 20058–20065
14 Bereiter-Hahn, J., Münnich, A. and Woitenek, P. (1998) Dependence of energy metabolism on the density of cells in culture. Cell Struct. Funct. **23**, 85–93
15 Glass-Marmor, L., Morgenstern, H. and Beitner, R. (1996) Calmodulin antagonists decrease glucose 1,6-bisphosphate, fructose 1,6-bisphosphate, ATP and viability of melanoma cells. Eur. J. Pharmacol. **313**, 265–271
16 Zwerschke, W., Mazurek, S., Massimi, P., Banks, L., Eigenbrodt, E. and Jansen-Dürr, P. (1999) Modulation of type M2 pyruvate kinase activity by the human papillomavirus type 16 E7 oncoprotein. Proc. Natl. Acad. Sci. U.S.A. **96**, 1291–1296
17 Wechsel, H. W., Petri, E., Bichler, K.-H. and Feil, G. (1999) Marker for renal cell carcinoma (RCC): The dimeric form of pyruvate kinase type M2 (Tu M2-PK). Anticancer Res. **19**, 2583–2590
18 Presek, P., Reinacher, M. and Eigenbrodt, E. (1988) Pyruvate kinase type M2 is phosphorylated at tyrosine residues in cells transformed by Rous sarcoma virus. FEBS Lett. **242**, 194–198
19 Eigenbrodt, E., Mazurek, S. and Friis, R. R. (1998) Double role of pyruvate kinase type M2 in the regulation of phosphometabolite pools. In Cell Growth and Oncogenesis (Bannasch, P., Kanduc, D., Papa, S. and Tager, J. M., eds.), pp. 15–30, Birkhäuser Verlag, Basel/Switzerland
20 Mazurek, S., Weisse, G., Wüst, G., Schäfer-Schwebel, A., Eigenbrodt, E. and Friis, R. R. (1999) Energy metabolism in the involuting mammary gland *in vivo*. **13**, 467–478
21 Thomas, S. and Fell, D. A. (1998) A control analysis exploration of the role of ATP utilisation in glycolytic-flux control and glycolytic-metabolite-concentration regulation. Eur. J. Biochem. **258**, 956–967
22 Wang, H. and Iynedjian, P. B. (1997) Acute glucose intolerance in insulinoma cells with unbalanced overexpression of glucokinase. J. Biol. Chem. **272**, 25731–25736
23 Teusink, B., Walsh, M. C., van Dam, K. and Westerhoff, H. V. (1998) The danger of metabolic pathways with turbo design. Trends Biochem. Sci. **23**, 162–169
24 Glass-Marmor, L. and Beitner, R. (1999) Taxol (paclitaxel) induces a detachment of phosphofructokinase from cytoskeleton of melanoma cells and decreases the levels of glucose 1,6-bisphosphate, fructose 1,6-bisphosphate and ATP. Eur. J. Pharmacol. **370**, 195–199
25 Peterkofsky, B. and Prather, W. (1982) Correlation between the rates of aerobic glycolysis and glucose transport, unrelated to neoplastic transformation, in a series of BALB 3T3-derived cell lines. Cancer Res. **42**, 1809–1816
26 zur Hausen, H. (1991) Human papilloma viruses in the pathogenesis of anogenital cancer. Virology **184**, 9–13
27 Davies, R., Hicks, R., Crook, T., Morris, J. and Vousden, K. (1993) Human papillomavirus type-16 E7 associates with a histone H2 kinase and with p102 through sequences necessary for transformation. J. Virol. **67**, 2521–2528
28 Massimi, P., Pim, D. and Banks, L. (1997) Human papilloma viruse type 16 E7 binds to the conserved carboxy-terminal region of the TATA box binding protein and this contributes to E7 transforming activity. J. Gen. Virol. **78**, 2607–2613
29 Chen, C. and Okayama, H. (1987) High efficiency transformation of mammalian cells by plasmid DNA. Mol. Cell. Biol. **7**, 2745–2752
30 Hugo, F., Mazurek, S., Zander, U. and Eigenbrodt, E. (1992) *In vitro* effect of extracellular AMP on MCF-7 breast cancer cells: Inhibition of glycolysis and cell proliferation. J. Cell. Physiol. **153**, 539–549
31 Bergmeyer, H. U. (1974) Methoden der enzymischen Analyse. 3, Band I und II, Verlag Chemie Weinheim/Bergstraße
32 Dixon, W. J. (1993) BMDP Statistical software manual. University of California Press, Los Angeles.
33 Phelps, W. C., Yee, C. L., Münger, K. and Howley, P. M. (1988) The human papillomavirus type 16 E7 gene encodes transactivation and transformation functions similar those of adenovirus EIA. Cell **53**, 539–547
34 Liu, Z., Ghai, J., Ostrow, R. S. and Faras, A. J. (1995) The expression levels of the human papillomavirus type 16 E7 correlate with its transforming potential. Virology **207**, 260–270
35 Dyson, N., Howley, P. M., Munger, K. and Harlow, E. (1989) The human papilloma virus 16 E7 oncoprotein is able to bind to the retinoblastoma gene product. Science **243**, 934–937
36 Weber, G., Stubbs, M. and Morris, H. P. (1971) Metabolism of hepatomas of different growth rates *in situ* and during ischemia. Cancer Res. **31**, 2177–2183

37 Snell, K. and Weber, G. (1986) Enzymic imbalance in serine metabolism in rat hepatomas. Biochem. J. **233**, 617–620
38 Verleysdonk, S., Martin, H., Willker, W., Leibfritz, D. and Hamprecht, B. (1999) Rapid uptake and degradation of glycine by astroglial cells in culture: synthesis and release of serine and lactate. Glia **27**, 239–248
39 Vriezen, N. and van Dijken, J. P. (1998) Fluxes and enzyme activities in central metabolism of myeloma cells grown in chemostat culture. Biotechnol. Bioeng. **59**, 28–39
40 Zerfass-Thome, K., Zwerschke, W., Mannhardt, B., Tindle, R., Botz, J. and Jansen-Dürr, P. (1996) Inactivation of the cdk inhibitor p27KIP 1 by the human papillomavirus type 16 E7 oncoprotein. Oncogene **13**, 2323–2330
41 Zwerschke, W. and Jansen-Dürr, P. (2000) Cell transformation by the E7 oncoprotein of the human papilloma virus type 16: interactions with nuclear and cytoplasmic target proteins Adv. Cancer Res. **78**, 1–29
42 Dröge, W., Eck, H.-P., Kriegbaum, H. and Mihm, S. (1986) Release of L-alanine by tumor cells. J. Immunol. **137**, 1383–1386
43 Tian, W.-N., Braunstein, L. D., Pang, J., Stuhlmeier, K. M., Xi, Q.-C., Tian, X. and Stanton, R. C. (1998) Importance of glucose-6-phosphate dehydrogenase activity for cell growth. J. Biol. Chem. **273**, 10609–10617
44 Rais, B., Comin, B., Puigjaner, J., Brandes, J. L., Creppy, E., Saboureau, D., Ennamany, R., Lee, W.-N. P., Boros, L. G. and Cascante, M. (1999) Oxythiamine and dehydroepiandrosterone induce a G1 phase cycle arrest in Ehrlich's tumor cells through inhibition of the pentose cycle. FEBS Lett. **456**, 113–118
45 Jacobson, M. K. and Jacobson, E. L. (1999) Discovering new ADP-ribose polymer cycles: protecting the genome and more. Trends Biochem. Sci. **24**, 415–417
46 West, D. K., Lenz, J. R. and Baglioni, C. (1979) Stimulation of protein synthesis and Met-tRNA$_f$ binding by phosphorylated sugars: Studies on their mechanism of action. Biochemistry **18**, 624–632
47 Brazill, D. T., Thorner, J. and Martin, S. (1997) Mck1, a member of the glycogen synthase kinase 3 family of protein kinases, is a negative regulator of pyruvate kinase in the yeast *Saccharomyces cerevisiae*. J. Bacteriol. **179**, 4415–4418
48 Kashiwaya, Y., Sato, K., Tsuchiya, N., Thomas, S., Fell, D. A., Veech, R. L. and Passonneau, J. V. (1994) Control of glucose utilization in working perfused rat heart. J. Biol. Chem. **269**, 25502–25514
49 Ryll, T. and Wagner, R. (1992) Intracellular ribonucleotide pools as a tool for monitoring the physiological state of *in vitro* cultivated mammalian cells during production processes. Biotechnol. Bioeng. **40**, 934–946

Received 17 October 2000/15 January 2001; accepted 6 March 2001